Muonic x-ray study of ^{199}Hg and ^{200}Hg

C. Günther,* E. B. Shera, M. V. Hoehn, and H. D. Wohlfahrt†
Los Alamos National Laboratory, Los Alamos, New Mexico 87545

R. J. Powers
Physics Department, California Institute of Technology, Pasadena, California 91125

Y. Tanaka
Department of Physics, Purdue University, West Lafayette, Indiana 47907

A. R. Kunselman
Department of Physics and Astronomy, University of Wyoming, Laramie, Wyoming 82071
(Received 30 August 1982)

Muonic x-ray spectra have been measured for ^{199}Hg and ^{200}Hg. From the data we have determined model-independent charge radii and isomer shifts of certain excited nuclear states and have inferred spectroscopic quadrupole moments of excited states for both isotopes. The quadrupole moment of the lowest $5/2^-$ state in ^{199}Hg is found to be positive, in agreement with previous muonic-atom data but in disagreement with a recent Mössbauer study. $B(E2)$ values of low-lying excited states have been determined for ^{199}Hg. An $E1$ muonic-nuclear resonance has been discovered in ^{200}Hg.

[NUCLEAR STRUCTURE ^{199,200}Hg; measured muonic x-ray spectra; deduced monopole and quadrupole charge parameters, isomer shifts.]

I. INTRODUCTION

The muonic x-ray spectra of the mercury isotopes have been studied previously with natural mercury targets[1–3] with emphasis on the investigation of muonic isomer shifts[2] and magnetic hyperfine interactions.[3] Recently Hahn *et al.*[4] measured the muonic $2p\rightarrow 1s$ (K x ray), $3d\rightarrow 2p$ (L x ray), and $4f\rightarrow 3d$ (M x ray) spectra of most stable mercury nuclei with isotopically separated targets. These authors studied both the nuclear monopole charge distribution and the static and dynamic quadrupole hyperfine effects. In spite of this investigation, some questions and inconsistencies remain. For example, in a recent Mössbauer study of the $(5/2)^-$ first excited state in ^{199}Hg, Wurtinger and Kankeleit[5] concluded that the quadrupole moment of this state is negative, in contrast to the result from the muonic work.[4] Another problem occurs in ^{200}Hg, for which Hahn *et al.*[4] observed inconsistent values for the $2p$ fine-structure splitting derived from analysis of the K and L x rays. A further surprising result is the strong excitation (12 ± 4%) of the first excited 2^+ state in ^{200}Hg reported by Link.[3] The direct dynamic $E2$ excitation leads to a population of less than 2% for the 2^+ level.[6]

We have measured the muonic x-ray spectra of ^{199,200,201}Hg with improved experimental accuracy compared to the work of Hahn *et al.*[4] This has allowed us to clarify the inconsistencies in ^{200}Hg and to give a more detailed discussion of the quadrupole hyperfine effects in ^{199}Hg. We present here the results of our analysis for ^{199,200}Hg. Analysis of the ^{201}Hg data is still in progress and the results will be published separately.

II. MEASUREMENTS AND EXPERIMENTAL RESULTS

The muonic x-ray measurements were performed at LAMPF using techniques described elsewhere.[7,8] The x-ray spectra from targets of the mercury isotopes and a ^{206}Pb target were measured simultaneously; the latter was used for energy calibration.[9] The isotopic purities of the mercury targets are listed in Table I.

The experimental spectrum of the L muonic x-ray lines for ^{199}Hg are shown in Fig. 1. The present

TABLE I. Properties and isotopic compositions of the Hg targets.

Isotope:	^{199}Hg	^{200}Hg
Chemical form:	oxide	oxide
Quantity:	16.4 g	9.6 g
	Isotopic composition (%)	
^{198}Hg	1.9	0.2
^{199}Hg	85.3	1.0
^{200}Hg	6.2	95.7
^{201}Hg	1.8	1.8
^{202}Hg	3.8	1.0
^{204}Hg	0.9	0.2

spectra represent about four times the amount of data and have twice the signal-to-noise ratio of the spectra of Hahn *et al.*[4] For ^{200}Hg, the energy region in the vicinity of the $2^+ \rightarrow 0^+$ nuclear γ ray is shown in Fig. 2. The muonic spectra were analyzed with the least-squares fitting procedure described elsewhere.[10] The energies and intensities of the observed transitions are given in Tables II and III, for muonic ^{199}Hg and ^{200}Hg, respectively. In the following paragraphs some aspects of the analysis will be discussed, stressing especially those features that differ from the analysis of Ref. 4.

The K and L x-ray spectra were analyzed by fitting the positions and intensities of *individual* spectral lines. These lines were then interpreted according to a theoretically computed line spectrum for each isotope. Each line was fitted with a Gaussian-convoluted Lorentzian line shape, the Lorentzian width in each case having been determined during the theoretical line spectrum computation. This procedure contrasts with that used for the odd-A isotopes in Ref. 4 in which a theoretically calculated spectrum is convoluted with a pure Gaussian response function, and then fitted directly to the experimental data. The energies of weak lines in the spectra produced by the isotopic impurities in the target were fixed at values determined in separate

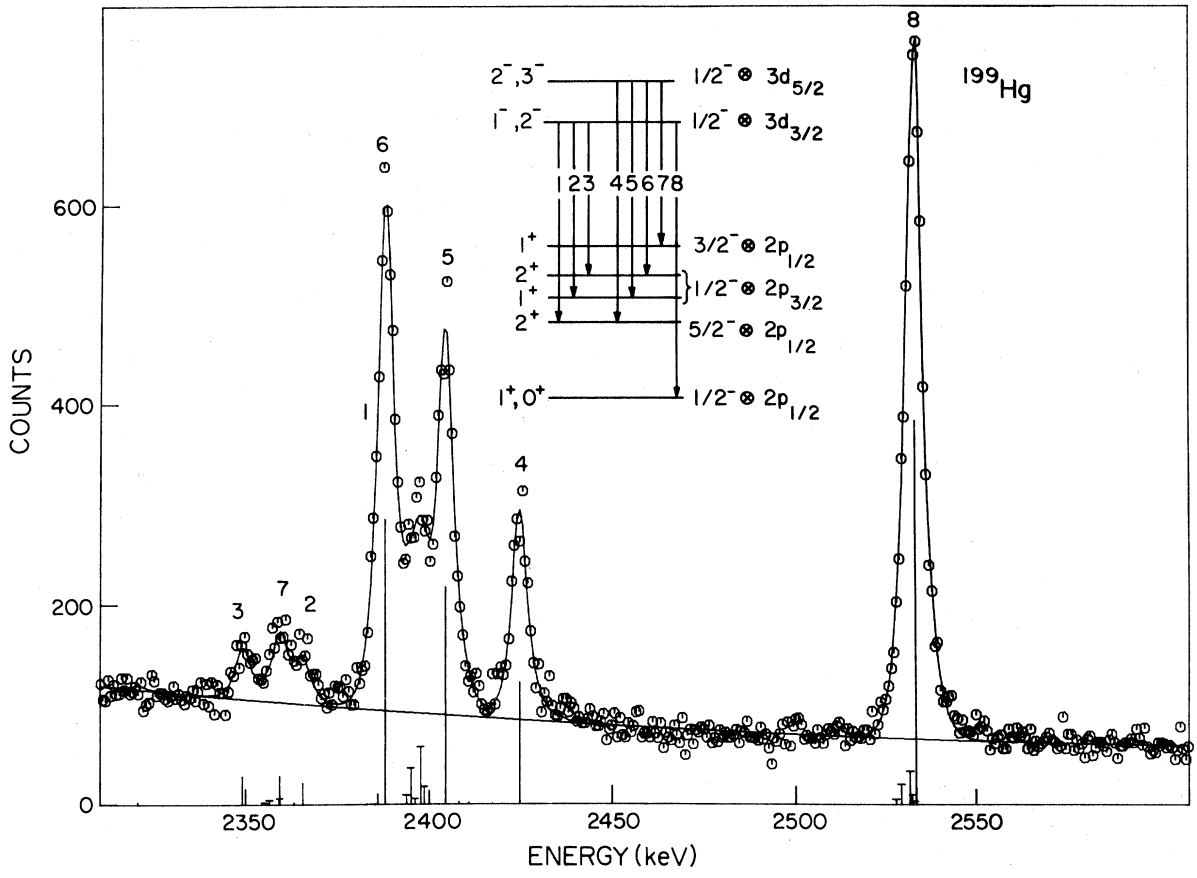

FIG. 1. Spectrum of the $3d \rightarrow 2p$ transitions observed for ^{199}Hg. The spectrum was measured with a large (10% efficiency) Ge(Li) detector with 5.7 keV FWHM at $E_\gamma = 5.7$ MeV. The capped vertical bars at the bottom of the figure indicate lines from other mercury isotopes.

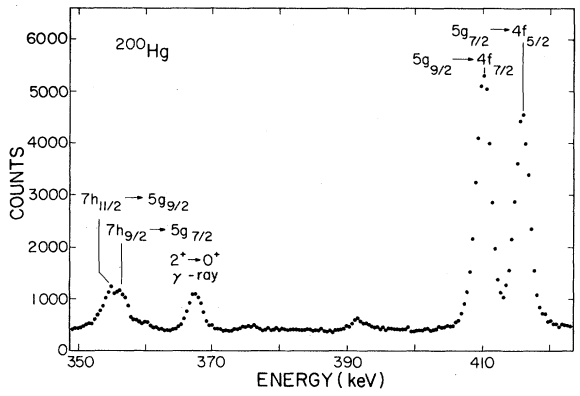

FIG. 2. Low-energy muonic x-ray spectrum of ^{200}Hg. The line at 367 keV is the $2^+ \rightarrow 0^+$ nuclear γ-ray transition.

measurements or, when necessary, taken from Ref. 4. The relative intensities of the isotopic impurities were fixed according to the known target composition. With the computer program of Akylas and Vogel,[11] we calculated the intensities of the K (95%), L (81%), and M (58%) lines; these values have been used for relative normalization of the observed intensities of the muonic x-ray transitions from the corresponding three regions of the spectrum.

In addition to the usual K and L lines, we observed, in the x-ray spectrum of ^{200}Hg, weak lines on the low-energy and high-energy sides of the $3d_{3/2} \rightarrow 2p_{1/2}$ and $2p_{1/2} \rightarrow 1s_{1/2}$ lines, respectively (see Fig. 3). These additional lines are interpreted as resulting from a $2p$-$1s$ muonic-nuclear resonance (see Sec. III E).

In concluding this section, we compare our spectral analysis with that of Hahn *et al.*[4] For ^{199}Hg we can only make an indirect comparison of the transition energies since only multiplet centroids are quoted in the earlier work. From the energies listed in Tables VI and XII of Ref. 4, one obtains

$$E(3d_{5/2} \rightarrow 1s_{1/2}) = 8236.7 \pm 0.2 \text{ keV} ,$$

whereas from the K and L x-ray transition energies in this work we obtain an average of 8236.3 ± 0.1 keV (the quoted errors are statistical only). The difference can be explained by the different calibration standards employed. Hahn *et al.*[4] used a weighted average of the Pb x-ray energies quoted in Ref. 12; these energies are approximately 0.3 keV higher than the Pb x-ray energy scale of Kessler *et al.*[9] which was used in our work. In the case of ^{200}Hg, we have included the x-ray energies of Ref. 4 in Table III for comparison with our results. Although there is satisfactory agreement for the L lines, the present K transition energies are smaller than those of Ref. 4 by 0.5 and 1.0 keV for the

TABLE II. Measured and calculated x-ray energies and intensities for muonic ^{199}Hg. Errors are given in parentheses. Both statistical uncertainties and total errors are given for the measured transition energies. Measured intensities of the $2p$-$1s$ transitions were arbitrarily normalized to 94.5%; intensities of the other transitions were determined by considering target self-absorption and relative detector efficiency. The calculated intensities were arbitrarily normalized to 94.5% for the $2p$-$1s$ transitions and the intensities of the other transitions were computed with the cascade program of V. R. Akylas and P. Vogel (California Institute of Technology Report CALT-63-600, 1978).

Transition[a]		Experimental		Calculated	
Initial state	Final state	Energy (keV)	Intensity (%)	Energy (keV)	Intensity (%)
$[(1/2)^- \otimes 2p_{3/2}]2^+$	$[(1/2)^- \otimes 1s_{1/2}]1^-$	5847.66 (13) (49)	17.7 (8)	5847.59	20.4
$[(1/2)^- \otimes 2p_{3/2}]1^+$	$[(1/2)^- \otimes 1s_{1/2}]0^-,1^-$	5831.66 (17) (54)	18.5 (10)	5831.56	18.7
$[(5/2)^- \otimes 2p_{1/2}]2^+$	$[(1/2)^- \otimes 1s_{1/2}]1^-$	5810.71 (56) (93)	4.0 (2)	5810.82	3.6
$[(1/2)^- \otimes 2p_{3/2}]2^+$	$[(5/2)^- \otimes 1s_{1/2}]2^-,3^-$	5688.96 (20) (46)	8.0 (4)	5689.13	7.3
$[(1/2)^- \otimes 2p_{1/2}]0^+,1^+$	$[(1/2)^- \otimes 1s_{1/2}]0^-,1^-$	5663.15 (9) (45)	34.1 (9)	5663.17	33.8
$[(5/2)^- \otimes 2p_{1/2}]2^+$	$[(5/2)^- \otimes 1s_{1/2}]2^-,3^-$	5652.56 (22) (58)	8.7 (5)	5652.24	8.3
$[(1/2)^- \otimes 2p_{3/2}]1^+$	$[(3/2)^- \otimes 1s_{1/2}]1^-,2^-$	5623.69 (37) (74)	3.5 (3)	5623.69	2.3
$[(1/2)^- \otimes 3d_{3/2}]1^-,2^-$	$[(1/2)^- \otimes 2p_{1/2}]0^+,1^+$	2534.16 (7) (9)	26.6 (8)	2534.16	28.7
$[(1/2)^- \otimes 3d_{5/2}]2^-,3^-$	$[(5/2)^- \otimes 2p_{1/2}]2^+$	2425.41 (12) (14)	9.3 (4)	2425.34	9.1
$[(1/2)^- \otimes 3d_{5/2}]2^-$	$[(1/2)^- \otimes 2p_{3/2}]1^+$	2404.86 (11) (13)	16.3 (6)	2404.88	16.3
$[(1/2)^- \otimes 3d_{5/2}]2^-,3^-$	$[(1/2)^- \otimes 2p_{3/2}]2^+$	2388.55 (9) (11)	22.4 (7)	2388.58	21.6
$[(1/2)^- \otimes 3d_{3/2}]1^-,2^-$	$[(1/2)^- \otimes 2p_{3/2}]1^+$	2366.23 (31) (31)	1.9 (4)	2365.93	1.4
$[(1/2)^- \otimes 3d_{5/2}]2^-$	$[(3/2)^- \otimes 2p_{1/2}]1^+$	2359.84 (41) (41)	2.4 (3)	2359.94	2.2
$[(1/2)^- \otimes 3d_{3/2}]1^-,2^-$	$[(1/2)^- \otimes 2p_{3/2}]2^+$	2349.94 (31) (31)	2.3 (3)	2349.65	1.9

[a]The listed assignments are those of the main configurations.

TABLE III. Measured and calculated energies and intensities of transitions observed in the muonic ^{200}Hg spectrum. See the caption of Table II.

Transition[a] Initial state	Final state	Experimental Energy (keV)	Intensity (%)	Calculated Energy (keV)	Intensity (%)	Reference 4 energy (keV)
$0^+\otimes 2p_{3/2}$	$0^+\otimes 1s_{1/2}$	5830.69 (8) (45)	60.5 (16)	5830.68	61.6	5831.19 (11) (52)
$1^-\otimes 1s_{1/2}$	$0^+\otimes 1s_{1/2}$[b]	5662.13 (97) (134)	3.6 (17)	5662.07	2.5	
$0^+\otimes 2p_{1/2}$	$0^+\otimes 1s_{1/2}$[b]	5657.41 (19) (56)	30.4 (19)	5657.44	30.4	5658.44 (16) (52)
$0^+\otimes 3d_{3/2}$	$0^+\otimes 2p_{1/2}$[b]	2532.60 (7) (9)	25.8 (8)	2532.60	25.9	2532.62 (14) (20)
$0^+\otimes 3d_{3/2}$	$1^-\otimes 1s_{1/2}$[b]	2528.04 (37) (39)	2.2 (4)	2527.94	2.1	
$0^+\otimes 3d_{5/2}$	$0^+\otimes 2p_{3/2}$	2398.30 (6) (7)	48.0 (10)	2398.31	48.2	2398.16 (10) (17)
$0^+\otimes 3d_{3/2}$	$0^+\otimes 2p_{3/2}$	2359.48 (17) (18)	5.0 (2)	2359.37	4.8	

[a]The listed assignments are those of the main configuration.
[b]Component of a partially resolved muonic-nuclear resonance line (see Fig. 3 and text).

$2p_{3/2}\rightarrow 1s_{1/2}$ and $2p_{1/2}\rightarrow 1s_{1/2}$ transitions, respectively. For the former line, the discrepancy is explained entirely by the different energy calibration standards. A residual difference remains for the $2p_{1/2}\rightarrow 1s_{1/2}$ line which presumably results from the neglect, in Ref. 4, of the close lying resonance line. This presumption is supported by the $2p_{3/2}$-$2p_{1/2}$ fine-structure splitting $\Delta 2p$ reported in Ref. 4. As already mentioned, Hahn *et al.*[4] obtained inconsistent values for $\Delta 2p$ from the K and from the L x rays. We find no such discrepancy. Taking

$$\Delta 3d = 38.87 \pm 0.06 \text{ keV},$$

we obtain

$$\Delta 2p = 173.28 \pm 0.21 \text{ keV}$$

and

$$173.17 \pm 0.11 \text{ keV}$$

from the K and L lines, respectively.

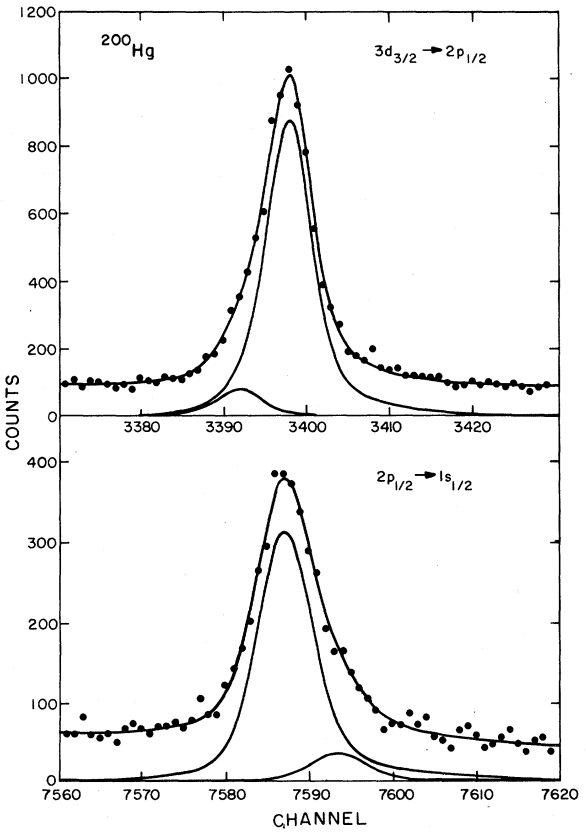

FIG. 3. Fit of doublets to the muonic $3d_{3/2}\rightarrow 2p_{1/2}$ and $2p_{1/2}\rightarrow 1s_{1/2}$ transitions in the muonic ^{200}Hg spectrum.

III. ANALYSIS

In this section, we discuss the monopole and the nuclear $E2$ moments that can be extracted from the muonic spectra. The theoretical basis of the present analysis has been discussed in detail in Refs. 7, 8, and 13. A brief summary of the procedures used in the analysis follows, after which we discuss the monopole and quadrupole results for both isotopes and the resonance observed in ^{200}Hg. Some measured nuclear properties used in the analysis are listed in Table IV.

A. Analysis of the monopole charge parameters

The eigenvalues of a muonic atom are determined in first order by the monopole interaction of the muon with the extended nuclear charge distribution and can be calculated by numerical solution of the Dirac equation[14] with an assumed model of the charge distribution. For the present analysis the nu-

TABLE IV. Nuclear properties of ^{199}Hg and ^{200}Hg from nonmuonic data. Except as indicated, values were obtained from Ref. 18.

Nucleus	Nuclear level			Transition		
	Energy (keV)	Spin (Parity)	Magnetic moment (μ_N)	I	I'	$B(E2;I\rightarrow I')$ (e^2fm^4)
^{199}Hg	0.0	$(1/2)^-$	+0.503			
	158.38 (1)	$(5/2)_1^-$	+1.04 (8)			
	208.20 (1)	$(3/2)_1^-$	0.52 (16)	5/2	$(3/2)_1$	601 (98)
	403.50 (4)	$(3/2)_2^-$		1/2	$(3/2)_2$	1640 (250)
	413.85 (8)	$(5/2)_2^-$		1/2	$(5/2)_2$	950 (160)
^{200}Hg	0.0	0^+				
	367.94 (1)	2^+	+0.84 (18)	0	2	8530[a] (70)

[a]Reference 28.

clear charge density in the body-fixed system was represented by a deformed Fermi distribution:

$$\rho(r,\theta)=\rho_0\left\{1+\exp\left[\frac{r-c(1+\beta Y_{20}(\theta))}{a}\right]^{-1}\right\}, \tag{1}$$

where c, a, and β are the half-density radius, surface thickness, and quadrupole deformation parameter, respectively. Corrections for higher-order quantum electrodynamic effects, electron screening, and nuclear polarization were calculated in the present analysis with methods described in Ref. 15.

In the analysis presented below for ^{199}Hg and ^{200}Hg, the nuclear monopole and certain quadrupole parameters were adjusted in a least-squares fitting procedure until the measured x-ray energies were reproduced. For comparison with Ref. 4, calculations were made with the value of the deformation parameter $\beta=0.0$, as well as with the value $\beta=-0.1$ in accord with the generally adopted deformation for the even mercury nuclei near $A=200$ (see, e.g., Ref. 16). Other parameters used in the analysis are given in Table IV. In the case of ^{199}Hg, additional small corrections for isomer shifts and magnetic hyperfine interactions were taken into account as described below.

The Barrett moment,[17] defined as

$$\langle r^k e^{-\alpha r}\rangle=\int\rho(r)r^k e^{-\alpha r}d^3r\ , \tag{2}$$

is a model-independent method of characterizing that particular property of the monopole charge distribution probed by a given muonic transition. The Barrett moment is derived from a parametrization of the muon-generated potential difference

$$\Delta V_\mu(r)=A+Br^k e^{-\alpha r}\ . \tag{3}$$

The parameters A, B, k, and α, which depend upon the nuclear and muonic states, are obtained by fitting the muon potential difference computed by numerical solution of the Dirac equation.

It is possible to consider that each muonic transition specifies a single model-independent radius parameter R_k, defined by

$$3R_k{}^{-3}\int_0^{R_k}r^k e^{-\alpha r}r^2dr=\langle r^k e^{-\alpha r}\rangle\ . \tag{4}$$

R_k is simply the radius of a sphere of constant charge density that has the value of the Barrett moment given by the right-hand side of Eq. (2).

Values of R_k and the Barrett moments determined from the present experiment are presented in Table V. The values of R_k determined for the $1s$ state are in agreement with those determined in Ref. 4, reflecting the agreement in the experimental $2p\rightarrow 1s$ transition energies.

The muonic isomer shift, which is related to the difference between the monopole charge distribution of an excited nuclear state and that of the ground state, is determined by comparing the excitation energy of the state in a muonic atom with the energy of the same state in a normal atom. A muonic isomer shift can be determined by either a direct measurement of the nuclear γ ray emitted while the muon is in the $1s$ state or by measurement of the difference in energies of certain K x rays.

In ^{199}Hg we have measured the isomer shifts for the first two excited states [$(5/2)^-$ and $(3/2)^-$] from the energies of the K x rays rather than from nuclear transitions as was done by Backe *et al.*[2] It has been shown that for both these nuclear levels there is considerable $M1$ internal conversion of the upper hyperfine component of the nuclear level due to the relatively long lifetime of the nuclear states. Hence, in order to obtain the isomer shifts using the nuclear transitions, it is necessary to determine the shift of the center of gravity of the (unresolved)

TABLE V. Model-independent monopole charge parameters of ^{199,200}Hg. ($\alpha = 0.1502$ fm^{-1}.) Errors (in parentheses) include both experimental errors and ambiguities in the dynamic $E2$ effect, but not ambiguities in nuclear-polarization corrections. See the text for an estimate of the influence of the latter. We note that all the R_k values are not entirely independent quantities since slight correlations involving the $2p$ states are introduced by extraction of the dynamic $E2$ effect. The sensitivity of the Barrett moments C_Z is $-(1/ZB)$ fm^k/keV.

Isotope	Transition	Energy[a] (keV)	B (keV/fm^k)	k	R_k (fm)	C_Z (fm/keV)	$\langle r^k e^{-\alpha r}\rangle$ (fm^k)
^{199}Hg	$2p_{3/2}$-$1s_{1/2}$	5841.02 (51)	1.323	2.3247	6.9610 (7)	-1.450×10^{-3}	21.482 (5)
	$2p_{1/2}$-$1s_{1/2}$	5665.60 (45)	1.308	2.3100	6.9599 (7)	-1.519×10^{-3}	20.940 (4)
	$3d_{3/2}$-$2p_{1/2}$	2531.81 (9)	1.041×10^{-2}	3.6210	7.0499 (9)	-1.009×10^{-2}	214.42 (11)
	$3d_{5/2}$-$2p_{3/2}$	2395.32 (12)	2.930×10^{-3}	4.0435	7.0768 (17)	-1.451×10^{-2}	461.9 (5)
	$3d_{3/2}$-$2p_{3/2}$	2356.39 (31)	2.927×10^{-3}	4.0381	7.076 (5)	-1.470×10^{-2}	457.3 (1.3)
	$1s_{1/2}$	10263.01[b] (57)	1.046	2.4645	6.9715 (8)	-1.319×10^{-3}	27.413 (7)
^{200}Hg	$2p_{3/2}$-$1s_{1/2}$	5834.84 (45)	1.321	2.3251	6.9700 (7)	-1.452×10^{-3}	21.538 (4)
	$2p_{1/2}$-$1s_{1/2}$	5659.77 (56)	1.306	2.3101	6.9688 (9)	-1.521×10^{-3}	20.984 (5)
	$3d_{3/2}$-$2p_{1/2}$	2530.37 (9)	1.033×10^{-2}	3.6232	7.0651 (9)	-1.008×10^{-2}	216.56 (11)
	$3d_{5/2}$-$2p_{3/2}$	2394.22 (7)	2.939×10^{-3}	4.0411	7.0935 (10)	-1.448×10^{-2}	463.30 (30)
	$3d_{3/2}$-$2p_{3/2}$	2355.29 (18)	2.947×10^{-3}	4.0340	7.0931 (26)	-1.466×10^{-2}	457.3 (8)
	$1s_{1/2}$	10255.70[b] (59)	1.041	2.4659	6.9814 (8)	-1.320×10^{-3}	27.541 (7)

[a]Effects due to $E1$ (for ^{200}Hg), $E2$, and $M1$ hyperfine splitting have been removed.
[b]Binding energy.

transitions due to the $M1$ conversion. This requires that one calculate both the conversion rate and the $M1$ hyperfine splitting of the excited level. Isomer shifts determined from the K x rays are free from such corrections since the $M1$ transition rate is negligible compared to the $E1$ muonic transition rate.

The present isomer shifts are presented, together with those determined previously, in Table VI. There is excellent agreement between the values for the $(5/2)^-$ level but very poor agreement for the $(3/2)^-$ level. This disagreement can be reduced by using the measured value[18] of the magnetic moment of the $(3/2)^-$ state ($\mu = 0.52\pm0.16\ \mu_N$) instead of the value ($\mu = -0.58\pm0.05\ \mu_N$) estimated by Backe *et al.*[12] from neighboring Hg isotopes. The Ref. 12 value of the isomer shift of the $(3/2)^-$ level would then become[19] 160^{+140}_{-90} eV, which is in somewhat better agreement with our value.

In ^{200}Hg, where there is too little dynamic $E2$ excitation for the K x-ray method to be useful, the isomer shift of the $(2^+\otimes 1s)$ state was determined by observation of the $2^+\rightarrow 0^+\gamma$ ray. In the analysis of this γ-ray line, we have taken into account the magnetic hyperfine splitting of the $(2^+\otimes 1s)$ state by fitting the spectrum with a doublet of lines, which we held fixed at the experimental intensity ratio[3] of

$$I_1/I_2 = 1.28\pm0.30\ .$$

In the fit the line width was held constant at an interpolated value determined from neighboring lines. The magnetic hyperfine splitting determined in this manner, $\Delta E = 460\pm210$ eV, is in fair agreement with the result of Link,[3] namely, 760 ± 180 eV. In any case, the centroid energy was constant within the experimental errors for any value of ΔE less than approximately 1 keV. We note that our result for the intensity of the $2^+\rightarrow 0^+$ γ-ray transition in ^{200}Hg (4.6 ± 0.5 %) is much smaller than the value of 12 ± 4 % quoted by Link.[3] A partial explanation for this discrepancy is that Link normalized his intensity using the result of a cascade calculation which gives an intensity of 68% for the N lines (see Table I

TABLE VI. Isomer shifts of nuclear excited states in ^{199,200}Hg determined from the present experiment and compared with those determined from other work.

Isotope	Nuclear state	Energy (keV)	Isomer shift (eV) Present experiment	Isomer shift (eV) Previous[a] measurements
^{199}Hg	$(5/2)^-$	158.38 (1)	270 (170)	265 (150)
	$(3/2)^-$	208.20 (1)	−560(380)	410 (120)
				$160\left[{}^{+140}_{-90}\right]$[b]
^{200}Hg	2^+	367.94 (1)	−390 (50)	−550 (200)

[a]Reference 12.
[b]Value recalculated using the experimental magnetic moment of the $(3/2)^-$ state and most recent $M1$ internal conversion coefficients (see text, Sec. III).

of Ref. 20). Renormalizing Link's experimental intensity with the results of the cascade calculation of Akylas and Vogel (58%), one obtains 10 ± 3%, which still differs appreciably from our result. The isomer shift determined from the present experiment, listed in Table VI, is in reasonable agreement with that of Link.[3]

B. Analysis of the quadrupole parameters

The muon in a muonic atom undergoes hyperfine interactions with the nuclear magnetic dipole and electric quadrupole moments. This leads to a splitting of the muonic states, for which, in heavy muonic atoms, the dominant effect is the quadrupole splitting in the $2p$ and $3d$ levels. In the present case, the ground-state static quadrupole hyperfine interaction vanishes, since the nuclear ground state spins of ^{199}Hg and ^{200}Hg are 1/2 and 0, respectively. However, both nuclei have low-lying nuclear states with energies comparable to the $2p_{3/2}$-$2p_{1/2}$ fine-structure splitting ($\Delta 2p$). The strong quadrupole interaction leads to mixing between muonic $2p$ states and nuclear levels. In the notation of Ref. 8, the quadrupole interaction matrix elements between the mixed muonic-nuclear states are given for the $2p$ muonic levels by

$$\langle IjF \mid H_Q \mid I'j'F\rangle=(-1)^{I'+F+j'-j+(1/2)}\left[\frac{4\pi}{5}(2j+1)(2j'+1)\right]^{1/2}\begin{Bmatrix} j' & I' & F \\ I & j & 2\end{Bmatrix}\begin{bmatrix} j' & 2 & j \\ 1/2 & 0 & -1/2\end{bmatrix}e^2W_{jj'}^{II'}\ , \tag{5}$$

where j and I are the muonic and nuclear angular momenta, $F=I+j$ is the total angular momentum of the muon-nucleus system, and

$$W_{jj'}^{II'}=\int \rho_{E2}^{II'}(r)V_{\mu}^{jj'}(r)r^2dr\ . \tag{6}$$

The weighting function $V_{\mu}^{jj'}(r)$ represents the quadrupole potential created by the muon at radius r, and $\rho_{E2}^{II'}(r)$ is the nuclear quadrupole charge density. The diagonal matrix element W_{jj}^{II} is related to the usual quadrupole hyperfine constant A_2 by

$$A_2=\sqrt{(\pi/5)}\frac{2j-1}{2j+2}\begin{bmatrix} I & 2 & I \\ -I & 0 & I\end{bmatrix}e^2W_{jj}^{II}\ . \tag{7}$$

Furthermore, it has been shown by numerical calculation[8] that the values for $W_{jj'}^{II'}$ involving the $2p_{1/2}$,$2p_{3/2}$ and $2p_{3/2}$,$2p_{3/2}$ muonic states differ by less than about 0.5%. The interaction between coupled muonic-nuclear states involving two different nuclear levels can then be approximately described by a single matrix element:

$$A_2^{II'}=\sqrt{(\pi/5)}\frac{2j-1}{2j+2}\begin{bmatrix} I' & 2 & I \\ -I' & I'-I & I\end{bmatrix}e^2W_{jj}^{II'}\ . \tag{8}$$

As discussed in Refs. 8 and 13, the diagonal and off-diagonal matrix elements $W_{jj}^{II'}$ can be related to the nuclear spectroscopic quadrupole moment $Q_s(I)$ and the reduced $E2$ transition probability $B(E2;I'\rightarrow I)$, respectively. This relationship involves the nuclear quadrupole charge or transition density of the states I and I'. In the present analysis we have assumed that the radial distribution of the quadrupole charge density is proportional, for all states, to

$$\int \rho(\hat{r})Y_{20}d\Omega\ ,$$

with $\rho(\hat{r})$ as given in Eq. (1). A detailed discussion of this assumption is given in Ref. 21.

C. Quadrupole interaction in ^{199}Hg

As demonstrated by Hahn *et al.*,[4] the structure of the muonic K and L spectra of ^{199}Hg is dominated by the splitting of the $2p$ levels due to dynamic quadrupole couplings to the two lowest excited states. In general, only a low-spin subset ($F^{\pi}=0^+,1^+,2^+$) of the members of the ($I^-\otimes 2p_{1/2,3/2}$) multiplet is observable in the experiment due to the low spin, $I^{\pi}=(1/2)^-$, of the ^{199}Hg ground state. This subset of states is shown in an insert in Fig. 1. Since only a limited number of states is observed, only a limited number of nuclear matrix elements can be determined from the experiment. We have been able to determine the $B(E2)$ values that connect the ground state and two lowest nuclear states and the quadrupole moments of these two states. The monopole parameters that could be determined are the ground-state Fermi distribution parameters c and a and the isomer shifts of the two lowest excited states. The fitted parameters are summarized in Table VII. Matrix elements that involve higher excited states were held constant in our analysis. The values of these fixed parameters were taken from the literature (see Table IV); for certain

TABLE VII. Nuclear charge and quadrupole parameters for ^{199}Hg, derived from fits to the K and L x rays. Except for the last column, the nuclear polarizations (NP) used were -4.027 keV $1s_{1/2}$, -1.555 keV $2p_{1/2}$, -1.415 keV $2p_{3/2}$, -0.126 keV $3d_{3/2}$, and -0.106 keV $3d_{5/2}$. Both $Q[(3/2)_2^-]$ and $Q[(5/2)_2^-]$ were held constant at zero. The uncertainties listed for fit I include only experimental errors; the uncertainties in fits II–V have similar values.

Parameter	Fit I[a] $\beta=-0.1$	Fit II[b] $\beta=-0.1$	Fit III[b] $\beta=0.0$	Fit IV[b] $\beta=0.0$ $t=2.3$ fixed	Fit V[b] $\beta=0.0$ Cole's NP[c]
c (fm)	6.6003 (54)	6.6005	6.6030	6.5697	6.6069
a (fm)	0.4930 (36)	0.4928	0.5015	0.5234 (fixed)	0.4999
$[(5/2)^-\otimes 1s]$ isomer shift (eV)	247 (175)	240	244	−33	−40
$[(3/2)^-\otimes 1s]$ isomer shift (eV)	−614 (385)	−623	−623	−89	−74
$B[E2;(1/2)^-\rightarrow(5/2)^-]$ (e^2fm^4)	3585 (53)	3659	3659	3911	3746
$B[E2;(1/2)^-\rightarrow(3/2)^-]$ (e^2fm^4)	1951 (61)	2037	2039	2205	2119
$Q[(5/2)^-]$ ($e$fm^2)	81 (9)	76	76	98	86
$Q[(3/2)^-]$ ($e$fm^2)	51 (9)	46	46	41	46

[a]With $B[E2;(5/2)_1^-\rightarrow(3/2)_2^-])=B[E2;(3/2)_1^-\rightarrow(3/2)_2^-]=B[E2;(3/2)_2^-\rightarrow(5/2)_2^-]=B[E2;(5/2)_1^-\rightarrow(5/2)_2^-]=B[E2;(3/2)_1^-\rightarrow(5/2)_2^-]=0$.

[b]With $B[E2;(5/2)_1^-\rightarrow(3/2)_2^-]$, $B[E2;(3/2)_1^-\rightarrow(3/2)_2^-]$, $B[E2;(3/2)_2^-\rightarrow(5/2)_2^-]$, $B[E2;(5/2)_1^-\rightarrow(5/2)_2^-]$, $B[E2;(3/2)_1^-\rightarrow(5/2)_2^-]$ as given in Ref. 22 [calculation labeled $B(E2)_{II}$].

[c]R. K. Cole, Jr., Phys. Rev. 177, 164 (1969).

transitions, no experimental $B(E2)$ values could be found. In these cases, we have used theoretical values[22] (see the footnotes of Table VII). An estimate of the influence of these particular fixed matrix elements can be obtained by comparing fit I in Table VII, for which the theoretically derived matrix elements have been set to zero, with fit II. The results of the two fits are generally consistent within the listed statistical errors.

We should note that the value we have used for the

$$B[E2;(5/2)_1^-\rightarrow(3/2_1^-)]$$

differs considerably from that used in Ref. 4, due to a new value for the $E2/M1$ mixing ratio of the 50 keV $(3/2)_1^-\rightarrow(5/2)_1^-$ transition. This value, which is derived from L-subshell conversion ratios, remains, however, somewhat uncertain due to possible penetration effects.[23] Magnetic hyperfine splitting effects were included in our calculations for the ground and two lowest excited states. The magnetic moments used in the $M1$ hyperfine calculation are those listed in Table IV normalized (reduced by 35%) so as to yield the observed value of the $[(1/2)^-\otimes 1s_{1/2}]$ splitting reported by Link.[3]

As is well known, the relative signs assumed for the $E2$ matrix elements can influence the parameters extracted from muonic levels. To investigate this effect we have performed several additional fits, the results of which are summarized below.

(1) Concerning the sign of the quadrupole moments, in all cases except those with positive values for the quadrupole moments of the $(5/2)_1^-$ and $(3/2)_1^-$ states, the fitted $B(E2)$ values differ greatly from nonmuonic results. For example, if the $(5/2)_1^-$ state is forced to have a negative quadrupole moment, then

$$B[E2;(1/2)^-\rightarrow(5/2)_1^-]$$

assumes a value which is more than ten standard deviations from the value of Ref. 18. We, therefore, reject the possibility of negative quadrupole moments for these states.

(2) Two possibilities exist for the signs of the $E2$ matrix elements between the three lowest nuclear states (see, e.g., Ref. 24). The results given in Table VII are for a positive

$$P_3=M_{1/2,5/2}\cdot M_{1/2,3/2}\cdot M_{5/2,3/2}\ .$$

For negative P_3, the fitted $B(E2)$ values are both approximately 10% smaller, which is in significant disagreement with the values determined by other

techniques. We therefore strongly favor P_3 positive.

(3) The difference in nuclear polarization ΔNP assumed for the two $2p$ states can have a significant effect on the extracted quadrupole parameters. We find for the derivatives with respect to ΔNP values of -37 $e^2\text{fm}^4/\text{keV}$, -306 $e^2\text{fm}^4/\text{keV}$, -18 $e\,\text{fm}^2/\text{keV}$, and -12 $e\,\text{fm}^2/\text{keV}$ for

$$B[E2;(1/2)\rightarrow(5/2)_1]\,,$$

$$B[E2;(1/2)\rightarrow(3/2)_1]\,,$$

$Q_s[(5/2)_1]$, and $Q_s[(3/2)_1]$, respectively.

Finally, for comparison with results of Hahn *et al.*,[4] we have performed several fits with $\beta=0$, with fixed surface thickness parameter $t=4\ln 3a=2.3$ fm, and with nonrelativistic nuclear polarization corrections. The results are listed in Table VII. As expected,[21] the use of a spherical ($\beta=0$) rather than a deformed Fermi distribution changes the ground-state monopole parameters c and a, but leaves the quadrupole parameters unaffected. When the skin thickness is fixed at 2.3 fm (fit IV in Table VII), the fit is no longer satisfactory and the parameter values change considerably in an attempt to accommodate to the arbitrarily constrained monopole energies. In the last column of Table VII, we list results of a fit using a nonrelativistic nuclear polarization (NP) calculation for which, among other differences, both $2p$ states have the same NP correction ($\Delta\text{NP}=0$) rather than $\Delta\text{NP}=140$ eV as in our standard analysis.

In general, the agreement of the present values for ^{199}Hg with those of Ref. 4 is satisfactory; the differences that exist can be understood to result largely from four areas in which Ref. 4 differs from the present analysis: (i) use of nonrelativistic NP corrections, (ii) neglect of the $(5/2)_2^-$ state in the analysis, (iii) fixed skin thickness parameter $t=2.3$ fm, and (iv) use of different fixed $B(E2)$ values in some cases.

D. Quadrupole interaction in ^{200}Hg

Of the low-lying nuclear levels in ^{200}Hg, all except the first 2^+ state have a negligible effect on the muonic levels due to their high excitation energies and small $B(E2)$ values. In fact, even this state is so weakly coupled in the muonic-nuclear system that only the two principal members of the $2p$ hyperfine multiplet of levels are observable. The extraction of any nuclear quadrupole information whatever from the muonic spectrum of ^{200}Hg thus must rest on the observed energy splitting of these two levels. Clearly only a single nuclear parameter can be extracted from the experiment. We have chosen to fit $Q(2^+)$, as did Hahn *et al.*,[4] simply because the other accessible parameter $[B(E2;0^+\rightarrow 2^+)]$ has been relatively well determined by Coulomb excitation experiments (see Table IV). The results of several fits, including two with $\beta=0$ and $t=2.3$ fm for comparison with Ref. 4, are given in Table VIII. The perturbation caused by the muonic resonance discussed in Sec. III E was accounted for by slight adjustment of the experimental energies used in the fits. The result we obtain for $Q(2^+)$ is essentially zero within the statistical error. The value is rather sensitive to the NP prescription used (see fit IV) and to the assumed $B(E2;0^+\rightarrow 2^+)$ value. Therefore an increase of 3% in the *effective* $B(E2)$ value, as might be expected to result from different but not unreasonable assumptions about $\rho_{E2}^{02}(r)$ in Eq. (6), changes the extracted quadrupole moment appreciably (see fit V). The rather large value deduced by Hahn *et al.*[4] presumably results from the use of a nonrelativistic NP correction and from the neglect of the $E1$ muonic-nuclear resonance in that work. In conclusion, the very weak muonic-nuclear quadrupole mixing for ^{200}Hg, together with uncertainties in the muonic analysis, prevents the extraction of a reliable value for the

TABLE VIII. Nuclear charge and quadrupole parameters for ^{200}Hg, derived from fits to the K and L x rays. The nuclear polarizations used were -4.146 keV $1s_{1/2}$, -1.608 keV $2p_{1/2}$, -1.466 keV $2p_{3/2}$, -0.124 keV $3d_{3/2}$, -0.102 keV $3d_{5/2}$. The $B(E2;0^+\rightarrow 2^+)$ was held constant at the value 8530 $e^2\text{fm}^4$ except for fit V, for which it was increased by 3%. The uncertainties listed for fit I include only experimental errors; the uncertainties in fits II–V have similar values.

Parameter	Fit I $\beta=-0.1$	Fit II $\beta=0.0$	Fit III $\beta=0.0$ $t=2.3$ fm (fixed)	Fit IV $\beta=0.0$ Cole's NP[a]	Fit V $\beta=-0.1$ $B(E2)=8786$
c	6.5848 (63)	6.5875	6.5798	6.6147	6.5831
a	0.5103 (40)	0.5185	0.5234 (fixed)	0.5014	0.5114
$Q(2^+)$ ($e\,\text{fm}^2$)	−4.5 (30.4)	−4.8	−4.3	+40.8	+17.4

[a]R. K. Cole, Jr., Phys. Rev. 177, 164 (1969).

quadrupole moment of the 2^+ state; identical considerations would apply to the other even isotopes of mercury.

E. Muonic resonance excitation in ^{200}Hg

As discussed above and illustrated in Fig. 3, we observed that the muonic lines populating and depopulating the $2p_{1/2}$ level in ^{200}Hg are doublets. The small components on the low-energy and high-energy sides of the L and K lines, respectively, can be understood to occur because of a $2p$-$1s$ resonance process involving a nuclear state with $I^\pi = 1^-$ at

$$E_{ex} \sim \Delta E(2p_{1/2} - 1s_{1/2}) \sim 5.6 \text{ MeV} .$$

Similar resonances have been reported in ^{172}Yb and ^{188}Os (Ref. 25); however, in these cases the resonance involved nuclear states near 3 MeV and the muonic $3d$ and $2p$ levels. In the present case, the nuclear ground state coupled to the $2p_{1/2}$ muonic level, $(0^+ \otimes 2p_{1/2})(1/2)^-$, apparently mixes with the $(1^- \otimes 1s_{1/2})(1/2)^-$ level, and this latter level is then populated from the $3d_{3/2}$ state via its $(0^+ \otimes 2p_{1/2})$ component (see, e.g., Ref. 25 and references given therein). From the observed branching ratio (0.085 ± 0.016) of the decay of the $3d_{3/2}$ level to the two mixed states and the observed level splitting $(4.6 \pm 0.4$ keV), one obtains both an energy shift δE of the two levels due to their interaction and the interaction matrix element M:

$$\delta E = 0.39 \pm 0.06 \text{ keV}$$

and

$$|M| = 1.26 \pm 0.14 \text{ keV} .$$

This implies that the nuclear state $(I^\pi = 1^-)$ must have an energy of 5661.6 ± 0.4 keV (neglecting isomer shift and magnetic hyperfine interaction). Furthermore, from the interaction matrix element M, one derives a reduced $E1$ transition probability of

$$B(E1; 0^+ \rightarrow 1^-) \sim 0.0315 \, e^2\text{fm}^2 ,$$

or approximately 0.01 Weisskopf units. In a recent photon scattering experiment, Laszewski and Axel[26] observed several 1^- levels with similar excitation energies in ^{208}Pb. These authors also performed measurements on natural mercury targets. They find a concentration of $E1$ strength near 5.5 MeV with a total $B(E1)$ of about 0.5 $e^2\text{fm}^2$. These photon scattering findings are not inconsistent with the parameters we deduce for the nuclear state involved in the muonic resonance.

From the observed intensities of the K and L lines (see Table III) that populate and depopulate the mixed $(1^- \otimes 1s_{1/2})$ and $(0^+ \otimes 2p_{1/2})$ levels, we conclude that for both states the majority of the depopulation occurs via the muonic channel rather than possible competing nuclear channels. In this connection, the intensity of the 367-keV $2^+ \rightarrow 0^+$ γ-ray transition that depopulates the first excited state is observed to be $4.6 \pm 0.5\%$ in the muonic spectrum (see Fig. 2). The intensity computed for this transition solely on the basis of the quadrupole $2p$ state mixing is 1.9%. It seems quite possible that the 2^+ state is also excited in the course of cascade transitions that result from occasional nuclear decay of the 1^- resonance state. In fact, a computation of the maximum reasonable 1^- state intensity that might feed into the excited nuclear states, based on the observed K and L x-ray intensities (and their probable errors) listed in Table III, yields 2.5%, a figure not inconsistent with the additional 2^+ state intensity observed. In view of the rather low intensity of the excitation and expected fragmentation of the γ decay of high-lying excited states, we would not expect to observe (and indeed we did not see) any individual γ-ray lines directly depopulating the 5.6-MeV state.

Hufner *et al.*[13] pointed out that one should not expect to observe resonances in heavy nuclei involving the $2p$ and $1s$ muonic states despite the fact that the density of nuclear compound states at an excitation energy of 6 MeV is already very high (about 10^4 states/MeV). It is proposed that this is a consequence of the smallness (less than 1 eV) of the interaction matrix element

$$\langle I_{ex} \otimes 1s_{1/2} | H | I_{gr} \otimes 2p_j \rangle ,$$

due to the complicated structure of the nuclear compound state involved (see the discussion on p. 294 of Ref. 13). However, as mentioned above, there is evidence[26] that in the elements near ^{208}Pb a few percent of the giant $E1$ strength remains at relatively low energies (5–7 MeV). According to theoretical calculations,[27] this $E1$ strength occurs as a small number of compound levels (a few per MeV); the predicted $B(E1)$ values of these levels correspond to muonic-nuclear resonance matrix elements of the order of 1 keV. In ^{200}Hg the observed resonance presumably involves such a level which happens to occur at an energy only a few keV from that of a muonic K transition. Curiously, a similar accidental resonance seems to occur in ^{202}Hg.[4]

IV. DISCUSSION OF QUADRUPOLE RESULTS

In Table IX we list what we consider to be the most probable experimental values of the $E2$ moments deduced from our data. The listed errors include uncertainties from several sources: statistical errors, uncertainties of correlated $E2$ moments held fixed in our analysis, and nuclear polarization uncertainties. Table IX also lists values determined previously from muonic atom,[4] Coulomb excitation,[16,28,29] Mössbauer,[5] and lifetime[18,23] measurements. There is excellent agreement between our $B(E2)$ values and those deduced from the lifetime measurements. The Coulomb excitation value is, however, somewhat larger than the present value. We have already alluded to the fact that the Mössbauer value of the quadrupole moment of the lowest state in ^{199}Hg disagrees in sign with the muonic values. We shall discuss this discrepancy further in the following subsections.

A. Quadrupole moment sign discrepancy

As mentioned above, Wurtinger and Kankeleit[5] derived a negative value for $Q[(5/2)^-]$ from their Mössbauer experiment, in contrast to the muonic result of Ref. 4. The authors of Ref. 5 suggest that the muonic result may be in error due to the neglect of a possible triaxial deformation of ^{199}Hg in the analysis of the muonic data. More recently, Saladin[30] suggested that there is also a discrepancy for the quadrupole moment of the 2^+ level in ^{198}Hg derived from Coulomb excitation reorientation and from muonic experiments, possibly connected to triaxiality. However, it was shown recently[21] that the γ deformation of the nucleus has a nearly negligible effect (less than 5%) on the extracted quadrupole parameters in ^{192}Os; the effects should be no larger in the *even* mercury isotopes. The application of a triaxial nuclear model to an odd-A nucleus is a more complex problem than it is for the collective states of an even-A nucleus since accurate knowledge of the Nilsson basis of the excited state wave functions is required in the former case for the prediction of transition densities. However, assuming the transition densities are surface-peaked, as is usual for low-lying excited states that have appreciable collective character, the muonic analysis would not be significantly affected by possible γ deformation of ^{199}Hg. It is certainly difficult to imagine a transition density that could *reverse the sign* of the extracted quadrupole moment. It therefore appears that the muonic results definitely establish a positive sign for the quadrupole moment of the $(5/2)^-$ level in ^{199}Hg. The positive sign is also supported by a β-γ perturbed angular correlation measurement[31] for the $(5/2)^-$ level in an Sb matrix, where the sign of the field gradient is known from nuclear orientation data.[32]

To explore other possible origins of the quadrupole moment discrepancy, we now discuss several uncertainties in the determination of the quadrupole moment $Q[(5/2)^-]$ using the Mössbauer technique. Wurtinger and Kankeleit[5] measured the quadrupole splitting $eQ[(5/2)^-]N_{zz}$ of the compound Hg_2F_2

TABLE IX. Comparison of the $E2$ moment results of the present experiment with those obtained from other experiments. Errors are indicated in parentheses and include uncertainties from several sources: statistical errors, uncertainties of correlated $E2$ moments held fixed in our analysis, and nuclear polarization uncertainties.

^{200}Hg	Present muonic atom	Previous[a] muonic atom	Coulomb excitation[b]	Coulomb excitation[c]	
$Q(2^+)$ e fm^2	10 (60)	260 (140)	107 (19)	111 (11)	
^{199}Hg	**Present muonic atom**	**Previous[a] muonic atom**	**Lifetime[d]**	**Coulomb excitation[e]**	**Mössbauer[f]**
$B[E2;(1/2)^-\rightarrow(5/2)^-]$ e^2fm^4	3620 (80)	3620 (100)	3670 (100)		
$B[E2;(1/2)^-\rightarrow(3/2)^-]$ e^2fm^4	2010 (85)	2160 (100)	2035 (210)	2410[g] (150)	
$Q[(5/2)^-]$ e fm^2	85 (12)	95 (6)			−80 (40)
$Q[(3/2)^-]$ e fm^2	50 (12)	62 (15)			

[a]Reference 4.
[b]Reference 28.
[c]Reference 16.
[d]Deduced from half-life and experimental internal conversion coefficient (Refs. 18 and 22).
[e]Reference 27.
[f]Reference 5.
[g]Relative measurement normalized to present value of $B[E2;(1/2)\rightarrow(5/2)]$.

and the alloy $Hg_{63}Pt_{37}$. In the Mössbauer, as in the muonic-atom, technique an interaction energy is measured. In order to interpret this energy in terms of a nuclear quadrupole moment, one must compute the electric field gradient with which the nuclear moment interacts. This field gradient (V) is due not only to the electrons (V_{el}) of the atoms to which the nucleus belongs, but also to other atoms in the vicinity (V_{lat}).

We believe that the interpretation of Wurtinger and Kankeleit[5] is perhaps the most reasonable, but definitely not the only, interpretation of the Mössbauer data. Figure 6 of Ref. 5 shows the Hg_2F_2 velocity spectrum on which the sign of the quadrupole moment, as determined from that compound, is based. The figure shows two peaks of nearly equal amplitude; since neither peak is clearly dominant, we suggest an acceptable fit to the data might be obtained for quadrupole moments of either sign. The Mössbauer data for the alloy, presented in Fig. 7 of Ref. 5, display an asymmetric pattern consisting of three peaks, which should establish the sign of the quadrupole interaction if the peaks have been properly identified.

However, the question of the reliability of the field gradient calculation for the alloy remains. The authors of Ref. 5 make use of the correlation between V_{el} and V_{lat} established by Raghavan *et al.*[33] for certain materials. Unfortunately, no such correlation has been established for $Hg_{63}Pt_{37}$. As a result, the authors infer the correlation from other mercury alloys. Since V_{lat} very nearly cancels V_{el}, the net field gradient is very sensitive to assumptions about the correlation.

B. Theoretical description of ^{199}Hg

Existing theoretical descriptions of the low-spin states in ^{199}Hg have not been entirely successful. Most theoretical work has been based on a particle-vibration coupling approach. In particular, Mathews *et al.*[22] performed a detailed theoretical investigation of ^{199}Hg within the framework of the intermediate coupling model. Their results for the electromagnetic properties of the three lowest states in ^{199}Hg are compared with the experimental values in Table X. The most significant disagreement is observed for $Q_s[(5/2)_1^-]$, where the calculation yields a negative value. More recently Wurtinger and Kankeleit[5] performed calculations within the framework of the asymmetric rotor model (see column four in Table X). Again their calculation gives a negative quadrupole moment for the $(5/2)_1^-$ level, which has been interpreted by these authors as support for their experimentally determined sign of $Q_s[(5/2)_1^-]$. However we would like to show here that the conventional strong coupling model with an axially symmetric oblate deformation gives rise to a positive $Q[(5/2)_1^-]$ in a straightforward fashion.

The strong coupling model with the particle-rotation coupling effect included[33–36] has been used in the following discussion. The Nilsson orbitals for the valence neutron have been constructed within the harmonic oscillator space of $N=5,6$ with the parameters $\kappa_n=0.0637$, $\mu_n=0.42$, and $\hbar\omega=41.2A^{-1/3}$ MeV. The inertial parameter $\hbar^2/2I=0.069$ MeV was taken from ^{198}Hg. The deformation parameter β_2 was assumed to be -0.13, which gives a reasonable excitation energy for the $(13/2)^+$ state. (This could be also achieved by adjusting κ or μ for the $N=6$ shell.) The pairing interaction G_n was fixed as $23/A$ MeV, which approximately reproduces the empirical gap energy from the mass tables.

Among the various parameters mentioned above, the most important in affecting the sign and the magnitude of the $Q[(5/2)_1^-]$ is found to be the difference in energy of the $1f_{5/2}$ and $2p_{1/2}$ spherical neutron single particle orbitals. When the $1f_{5/2}$ orbital (which is typically assumed to be 1 MeV lower

TABLE X. Comparison of experimental electromagnetic properties of the three low-lying states in ^{199}Hg with predictions of the intermediate coupling model,[a] the asymmetric rotor model,[b] and the present strong coupling calculation.

Parameter	Experiment	Intermediate coupling	Asymmetric rotor	Strong coupling
$B[E2;(1/2)\rightarrow(5/2)]$ e^2fm^4	3620 (80)	1920	4650	4320
$B[E2;(1/2)\rightarrow(3/2)]$ e^2fm^4	2010 (85)	1540		3050
$B[E2;(5/2)\rightarrow(3/2)]$ e^2fm^4	601 (100)	9		630
$Q(5/2)$ e fm^2	85 (12)	-73	-90	75
$Q(3/2)$ e fm^2	50 (12)	54		25

[a]Reference 21.
[b]Reference 5.

than the $2p_{1/2}$ orbital) is close to or above the $2p_{1/2}$ orbital, the $(5/2)_1^-$, 0.158-MeV state is predicted to be a member of the (5/2)[503] (Ref. 37) rotational band, while the $(5/2)_2^-$, 0.414-MeV state is a member of the (1/2)[521] ground-state rotational band. In this case, the calculation predicts that the ratio R of the $B(E2)$ from the $(1/2)^-$ ground state to these two $(5/2)^-$ states,

$$R=\frac{B[E2;(1/2)^-\rightarrow(5/2)_1^-]}{B[E2;(1/2)^-\rightarrow(5/2)_2^-]}\ ,$$

would be much less than unity. On the other hand, when the $1f_{5/2}$ orbital is assumed to be lower than the $2p_{1/2}$ orbital, the roles of the two 5/2 states are reversed. To illustrate this situation in more detail, the quadrupole moments, $Q[(5/2)_1^-]$ and $Q[(5/2)_2^-]$, and the $B(E2)$ values,

$$B[E2;(1/2)^-\rightarrow(5/2)_1^-]$$

and

$$B[E2;(1/2)^-\rightarrow(5/2)_2^-]\ ,$$

have been calculated and plotted with respect to the single particle energy difference

$$\Delta E(f-p)=E(1f_{5/2})-E(2p_{1/2})$$

in Fig. 4. The $1f_{7/2}$ orbital has been shifted along with the $1f_{5/2}$ orbital to maintain a fixed spin-orbit energy.

The figure shows that the $Q[(5/2)_1^-]$ varies from -1.26 e b for $\Delta E(f-p)=0.0$ MeV to $+0.73$ e b for $\Delta E(f-p)=-2.8$ MeV, and the $B(E2)$ ratio R varies from 0.02 for $\Delta E(f-p)=0.0$ MeV to 36 for $\Delta E(f-p)=-2.8$ MeV. By using the experimental value[18,22] $R=38$ for the $B(E2)$ ratio, which corresponds to $\Delta E(f-p)=-1.8$ MeV, we obtain $Q[(5/2)_1^-]=0.75$ e b as shown in Table X. The calculated energies compare with experiment (in brackets) as follows:

$$E[(3/2)_1^-]=0.05\ [0.21]\ \text{MeV}\ ,$$

$$E[(3/2)_2^-]=0.34\ [0.40]\ \text{MeV}\ ,$$

$$E[(5/2)_1^-]=0.04\ [0.16]\ \text{MeV}\ ,$$

$$E[(5/2)_2^-]=0.53\ [0.41]\ \text{MeV}\ ,$$

and

$$E[(13/2)_1^+]=0.59\ [0.53]\ \text{MeV}\ .$$

The calculated magnetic moments (compared with experiment) are the following:

$$\mu[(1/2)^-]=0.66\ [0.51]\ \mu_N\ ,$$

$$\mu[(5/2)^-]=1.10\ [1.04]\ \mu_N\ ,$$

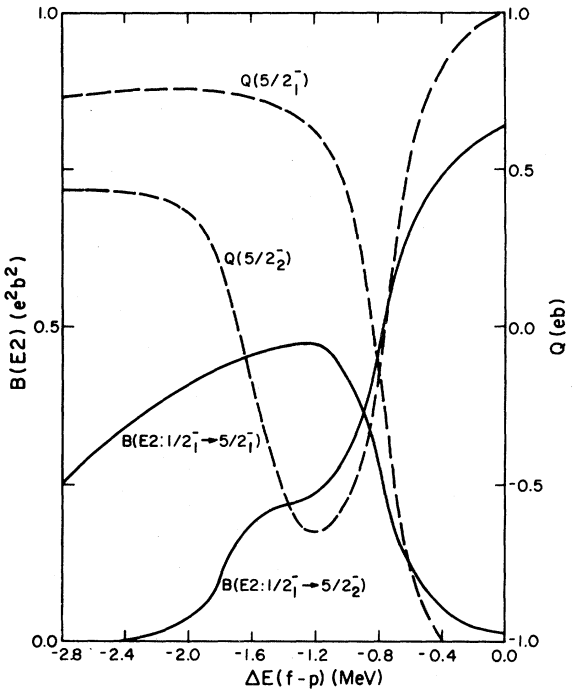

FIG. 4. Calculated $E2$ moments of the two lowest $(5/2)^-$ states in ^{199}Hg plotted as a function of the difference in energy $[E(f-p)]$ of the $1f_{5/2}$ and $2p_{1/2}$ Nilsson levels. Other relevant single particle energies (in MeV) were taken to be the following: $0i_{13/2}=1.06$, $2p_{3/2}=2.95$, $2p_{1/2}=4.30$, and $1f_{5/2}-1f_{7/2}=3.15$. Details of the calculation, which is based on the strong coupling model including particle-rotation coupling effects, are discussed in the text.

and

$$\mu[(3/2)^-]=-0.60\ [0.52]\ \mu_N\ .$$

The agreement between calculation and experiment seems satisfactory.

The calculations of Mathews *et al.*[22] and Wurtinger and Kankeleit[5] assumed, contrary to the customary level ordering,[38] a $1f_{5/2}$ single particle energy which is 400 keV *higher* than the $2p_{1/2}$ orbital. This value of the single particle energy seems to have been introduced to obtain better calculated energies for the low-lying states of ^{199}Hg. However, this procedure also produces an interchange of the wave functions between the first and the second excited $(5/2)^-$ states, yielding the negative quadrupole moment for the $(5/2)_1^-$ state as well as a $B(E2)$ ratio R that is less than unity in the calculation of Ref. 22. The same situation may exist in the calculation of Ref. 5, though the quadrupole moment of the $(5/2)_2^-$ state and the $B(E2)$ value between the ground state and the $(5/2)_2^-$ state are not reported in that work.

It is worthwhile to note that the quadrupole moment of the $(5/2)^-_1$, 0.134-MeV state in ^{197}Hg is reported to be $-0.081\ e$ b.[39] This sudden change of quadrupole moment between neighboring Hg isotopes[40] may also be understood from the present calculation. Taking the $B(E2)$ value of ^{197}Hg from the lifetime measurement,[40]

$$B[E2;(1/2)^-_1 \rightarrow (5/2)^-_1] = 0.28\ e^2b^2\ ,$$

we obtain from Fig. 4

$$Q[(5/2)^-_1] = -0.14\ e\,\text{b}\ .$$

The single-neutron-transfer data,[41] especially from the (d,t) experiment, may suggest that two different intrinsic configurations are involved in the low-lying states of ^{199}Hg. However, such an interpretation seems inconsistent with the observed

$$B[E2;(1/2)^- \rightarrow (5/2)^-]$$

value, which would be predicted to be an order of magnitude smaller by calculations forced to reproduce the reported (d,t) spectroscopic factors. The origin of this inconsistency is unknown, but may reflect the difficulty involved in transfer reaction studies on a volatile target such as Hg.

V. SUMMARY

We have presented here the results of our analysis of the muonic spectra of ^{199}Hg and ^{200}Hg. Improved experimental data and a more realistic line shape representation allowed us to resolve the previously reported[4] discrepancy associated with the fine structure splitting in ^{200}Hg by identification of an $E1$ resonance in that nucleus. A further investigation of resonance effects in ^{202}Hg as well as ^{200}Hg would be interesting, since the muonic-atom technique provides a unique opportunity to determine precise energies and $B(E1)$ values for certain compound nuclear levels.

Our analysis for ^{199}Hg essentially confirms the findings of the earlier muonic experiment.[4] Specifically we are not able to support the negative value of the quadrupole moment of the $(5/2)^-$ state inferred from the Mössbauer experiment. A theoretical calculation based on the strong coupling model is in fact consistent with a positive quadrupole moment for this state.

We would like to thank E. Bovet, M. E. Bunker, A. Forster, G. M. Kalvius, and P. Vogel for valuable discussions.

---

*Permanent address: Physicalisches Institüt der Universität Bonn, *D*-53 Bonn, Federal Republic of Germany.

†Deceased.

[1]H. L. Acker, G. Backenstoss, C. Daum, J. C. Sens, and S. A. DeWit, Nucl. Phys. 87, 1 (1966).

[2]H. Backe, R. Engfer, E. Kankeleit, R. Link, R. Michaelsen, C. Petitjean, L. Schellenberg, H. Schneuwly, W. U. Schroder, J. L. Vuilleumier, H. K. Walter, and A. Zehnder, Nucl. Phys. A234, 469 (1974).

[3]R. Link, Z. Phys. 269, 163 (1974).

[4]A. A. Hahn, J. P. Miller, R. J. Powers, A. Zehnder, A. M. Rushton, R. E. Welsh, A. R. Kunselman, P. Roberson, and H. K. Walter, Nucl. Phys. A314, 361 (1979).

[5]W. Wurtinger and E. Kankeleit, Z. Phys. A 293, 219 (1979).

[6]H. K. Walter, Nucl. Phys. A234, 504 (1974).

[7]E. B. Shera, E. T. Ritter, R. B. Perkins, G. A. Rinker, L. K. Wagner, H. D. Wohlfahrt, G. Fricke, and R. M. Steffen, Phys. Rev. C 14, 731 (1976).

[8]L. K. Wagner, E. B. Shera, G. A. Rinker, and R. K. Sheline, Phys. Rev. C 16, 1549 (1977).

[9]D. Kessler, H. Mes, A. C. Thompson, H. L. Anderson, M. S. Dixit, C. K. Hargrove, and R. J. McKee, Phys. Rev. C 11, 1719 (1975).

[10]E. B. Shera, M. V. Hoehn, L. K. Wagner, Y. Yamazaki, R. M. Steffen, and K. S. Krane, Phys. Lett. 67B, 26 (1977).

[11]V. R. Akylas and P. Vogel, Comput. Phys. Commun. 15, 291 (1978).

[12]R. Engfer, H. Schneuwly, J. L. Vuilleumier, H. K. Walter, and A. Zehnder, At. Data Nucl. Data Tables 14, 509 (1974).

[13]J. Hufner, F. Scheck, and C. S. Wu, in *Muon Physics,* edited by V. W. Hughes and C. S. Wu (Academic, New York, 1977), Vol. 1, p. 201.

[14]G. A. Rinker, Comput. Phys. Commun. 16, 221 (1979).

[15]Y. Yamazaki, E. B. Shera, M. V. Hoehn, and R. M. Steffen, Phys. Rev. C 18, 1474 (1978).

[16]A. Bockisch, K. Bharuth-Ram, A. M. Kleinfeld, and K. P. Lieb, Z. Phys. A 291, 245 (1979).

[17]R. C. Barrett, Phys. Lett. 33B, 388 (1970).

[18]J. Halperin, Nucl. Data Sheets 24, 57 (1978); M. R. Schmorak, *ibid.* 26, 81 (1979).

[19]H. K. Walter, private communication.

[20]H. Backe, R. Engfer, U. Jahnke, E. Kankeleit, R. M. Pearce, C. Petitjean, L. Schellenberg, H. Schneuwly, W. U. Schroder, H. K. Walter, and A. Zehnder, Nucl. Phys. A189, 472 (1972).

[21]M. V. Hoehn, E. B. Shera, H. D. Wohlfahrt, Y. Yamazaki, R. M. Steffen, and R. K. Sheline, Phys. Rev. C 24, 1667 (1981).

[22]G. J. Mathews, F. M. Bernthal, and J. D. Immele, Phys. Rev. C 11, 587 (1975).

[23]O. Dragoun, V. Brabec, M. Rysavy, and A. Spalek, Z. Phys. A 281, 347 (1977).

[24]K. Kumar, Phys. Lett. 29B, 25 (1969).

[25]M. V. Hoehn and E. B. Shera, Phys. Rev. C 20, 1934

(1979).
[26]R. M. Laszewski and P. Axel, Phys. Rev. C 19, 342 (1979).
[27]M. Harvey and F. C. Khanna, Nucl. Phys. A221, 77 (1974).
[28]R. Kalish, R. R. Borchers, and H. W. Kugel, Nucl. Phys. A161, 637 (1970).
[29]R. H. Spear, M. T. Esat, M. P. Fewell, D. C. Kean, T. H. Zabel, A. M. Baxter, and S. Hinds, Nucl. Phys. A345, 252 (1980).
[30]J. X. Saladin, Nucl. Phys. A347, 231 (1980).
[31]K. Krien and P. Herzog, private communication.
[32]J. C. Soares, K. Krien, P. Herzog, H.-R. Folle, K. Freitag, F. Reuschenbach, M. Reuschenbach, and R. Trzcinski, Z. Phys. B 31, 395 (1978).
[33]R. S. Raghavan, E. N. Kaufmann, and P. Raghavan, Phys. Rev. Lett. 34, 1280 (1975).
[34]Y. Tanaka and R. K. Sheline, Nucl. Phys. A276, 101 (1977).
[35]M. E. Bunker and C. W. Reich, Rev. Mod. Phys. 43, 348 (1971).
[36]W. Ogle, S. Wahlborn, R. Piepenbring, and S. Fredriksson, Rev. Mod. Phys. 43, 424 (1971).
[37]Following the usual convention, we use the Nilsson quantum numbers defined for the prolate deformed region to label both oblate and prolate Nilsson states.
[38]S. G. Nilsson, C. F. Tsang, A. Sobiczewski, Z. Szymanski, S. Wycech, C. Gustafson, I.-L. Lamm, P. Moller, and B. Nilsson, Nucl. Phys. A131, 1 (1969); R. A. Sorensen, in *Proceedings of the Fourth International Conference on Nuclei Far from Stability, Helsingør, Denmark, 1981,* edited by P. G. Hansen and G. B. Nielsen (CERN, Geneva, 1981).
[39]P. Herzog, K. Krien, K. Freitag, M. Reuschenbach, and H. Walitzki, Nucl. Phys. (to be published).
[40]K. Krien, R. Trzcinski, and F. Reuschenbach, Hyp. Int. 9, 105 (1981).
[41]R. A. Moyer, Phys. Rev. C 5, 1678 (1972).